

Use of Coupled Multi-Electrode Arrays to Advance the Understanding of Selected Corrosion Phenomena

N. D. Budiansky, F. Bocher, H. Cong, M. F. Hurley, and J. R. Scully

Center for Electrochemical Science and Engineering
Department of Materials Science and Engineering
University of Virginia
116 Engineer's Way
Charlottesville, VA, USA 22904



Acknowledgements

- The concrete project was sponsored by the VTRC (Virginia Transportation Research Council). The support and helpful discussions with Dr. Gerardo Clemeña and Dr. Steve Sharp are gratefully acknowledged.
- The crevice corrosion work was supported by the Office of Science and Technology International (OST&I), Office of Civilian Radioactive Waste Management, U.S. Department of Energy.
- Dr. Harold T. Michels and Copper Development Association Inc. provided financial support for pitting of Cu studies.
- The United States Department of Energy, Office of Basic Energy Sciences, Division of Materials Sciences and Engineering supported intergranular corrosion studies under contract DEFG02-00ER45825 with Jane Zhu as contact monitor.
- Special thanks to Scribner Associates, Inc. for instrument and software support.
- **The views, opinions, findings, and conclusions or recommendations of authors expressed herein do not necessarily state or reflect those of the DOE/OCRWM/OST&I.**

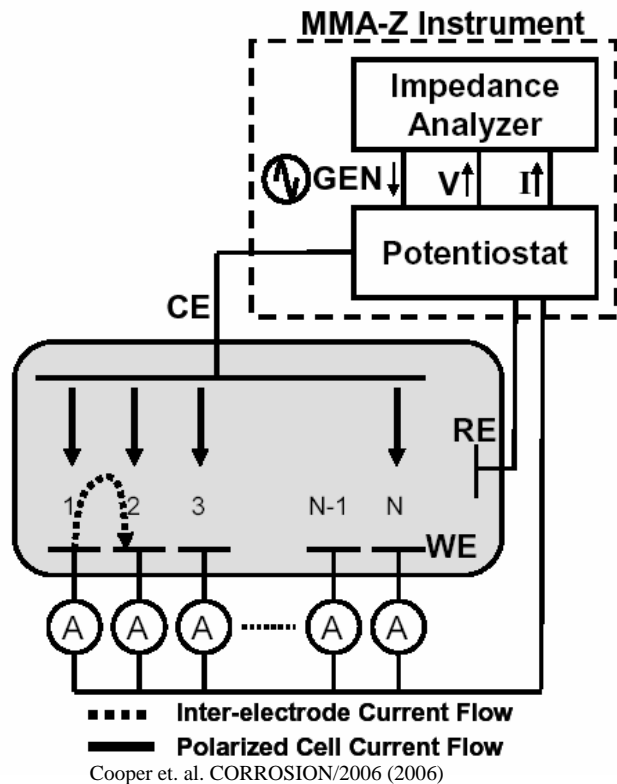
Local Electrochemical Processes

- Local electrochemical processes differ significantly from global process averaged over entire surfaces.
- Many methods exist to probe local processes:
 - Scanning or localized EIS
 - Scanning vibrating probe
 - **Multi-Electrode Arrays**
 - Scanning electrochemical microscopy

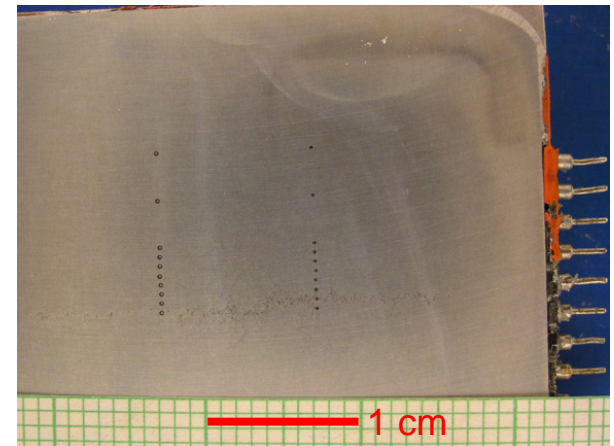
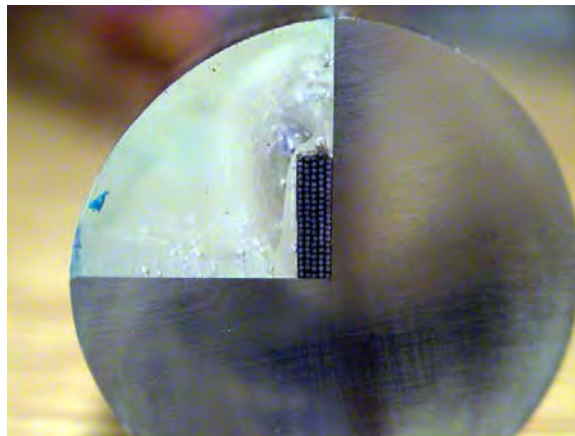
Motivation for Using Coupled Electrode Arrays

- High throughput
- Enhanced understanding of corrosion mechanisms
 - Triggering of corrosion modes by others
 - Cooperative spreading of corrosion
 - Spatial resolution and distribution (local anodes and cathodes)
 - Conditions for persistent anode development
 - Interrogation of electrochemical properties at specific locations
- Monitoring in field

Coupled Multi-Electrode Arrays

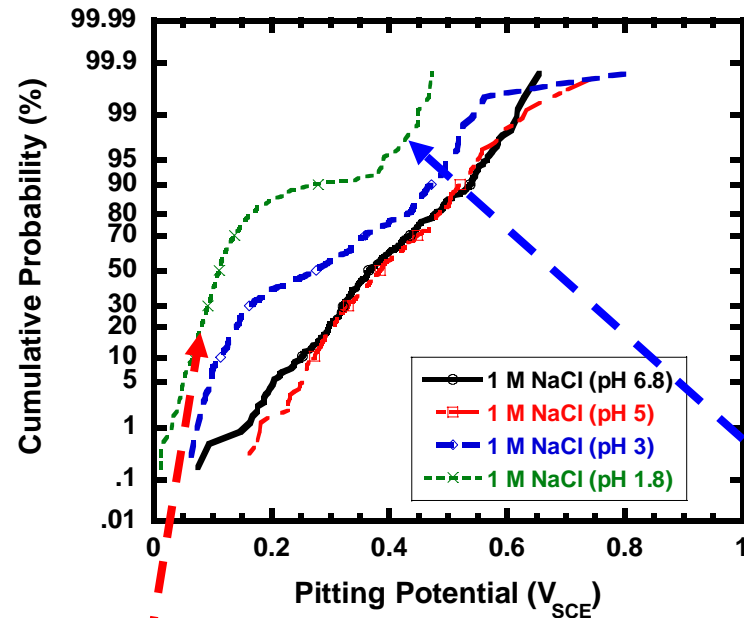


- Constructed from nominally identical electrodes or a combination of different materials to simulate compositional and structural heterogeneous surfaces. (i.e., Al-Cu)
- Allow temporal and spatial measurements of electrochemical processes simultaneously
- **Far Spaced MEAs** – Allow high throughput experiments
 - Eliminates variations in test environment
- **Close spaced MEAs** - Simulates a planar electrode
 - Electrodes close enough to allow chemical and electrochemical coupling of electrodes
- **Embedded Sensor MEAs** – monitor behavior of corrosion on a planar electrode surface.



Far Spaced Electrodes: High Throughput Testing

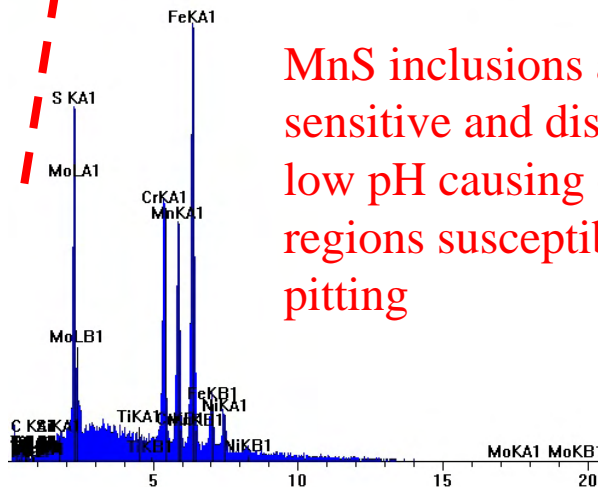
- Materials have a statistical distribution of flaws that control electrochemical properties (i.e., pitting potential). Causes distribution in E_{pit} .
- High throughput testing elucidates information about different portions of the underlying microstructure.



AISI 316 SS in 1 M NaCl 47°C

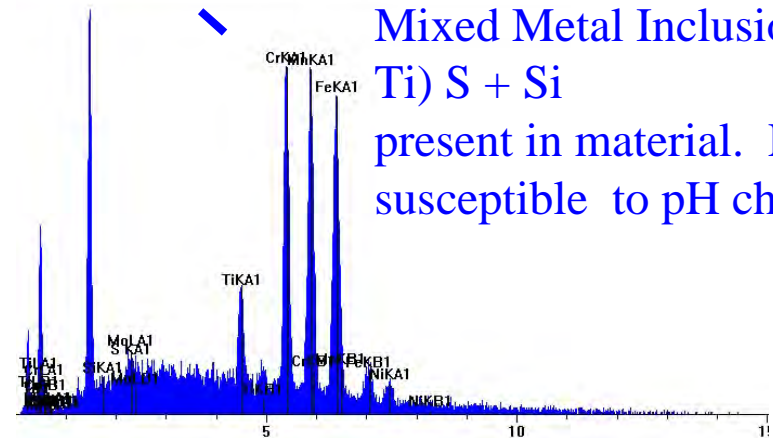
EDS_012406008.jpg

FS: 1100



MnS inclusions are pH sensitive and dissolve at low pH causing occluded regions susceptible to pitting

012406004.jpg



Mixed Metal Inclusions (Mn, Ti) S + Si present in material. Less susceptible to pH changes.

Potential Coupling

Potential Coupling through electrolyte phase through ohmic potential fields

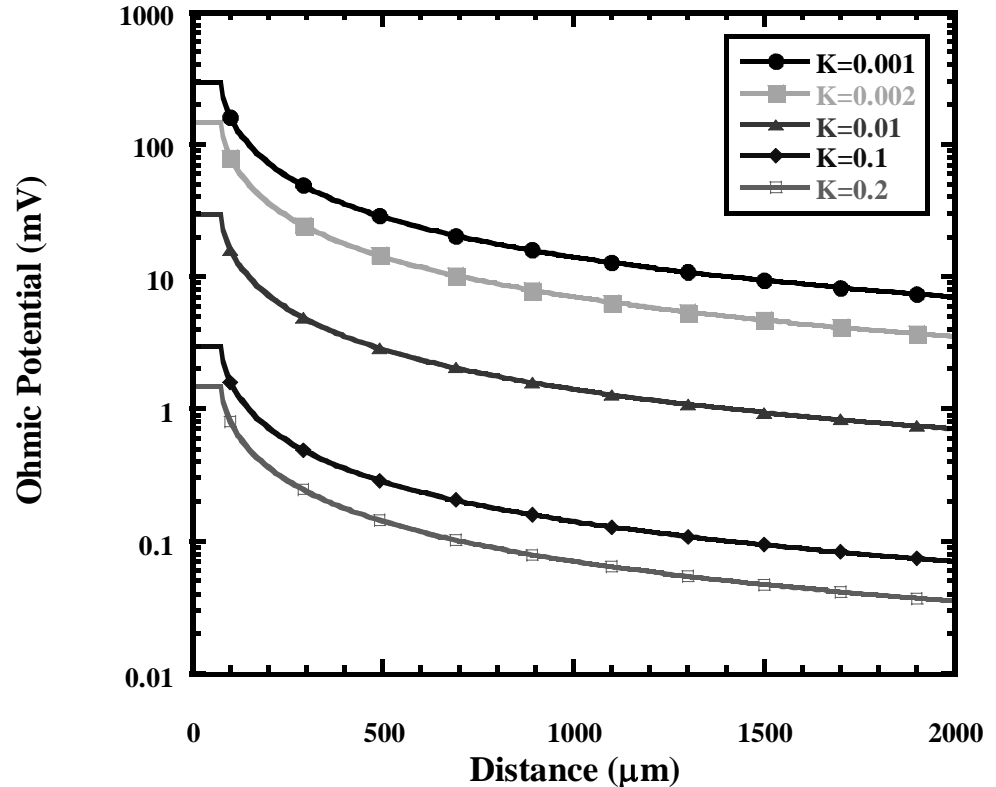
$$E_{\text{Applied/Measured}} = E_{\text{Interface}} + V_{\text{Ohmic}}$$

The Ohmic Potential can be predicted using Newman's solution:

$$\frac{\Phi}{\Phi_0} = 1 - \left(\frac{2}{\pi}\right) \cdot \tan^{-1}(\xi)$$

$$I = 4K \cdot r_0 \cdot \Phi_0$$

$$r = r_0 \cdot \sqrt{(1 + \xi^2) \cdot (1 - \eta)^2}$$



Φ =Ohmic potential (V)

Φ_0 =Maximum ohmic potential (V)

ξ =Distance from center of disk, in elliptical coordinates (cm)

η =Second elliptical coordinate (in this case = 0)

r = Normalized distance from center of disk (cm)

I =Total current from disk (A)

K =Solution conductivity ($\Omega^{-1}\text{-cm}^{-1}$)

r_0 =Radius of electrode (cm)

Chemical Coupling

Regions in the vicinity of electrochemically active sites where hydrolysis occurs.

Chemical gradients predicted by Carslaw and Jaeger:

$$\frac{C_r}{C_{pit}} = \frac{a}{r} * \operatorname{erfc}\left(\frac{r-a}{2\sqrt{Dt}}\right)$$

Where:

C_r = concentration at a distance r from the pit mouth (Moles/l)

C_{pit} = concentration inside the pit (Moles/l)

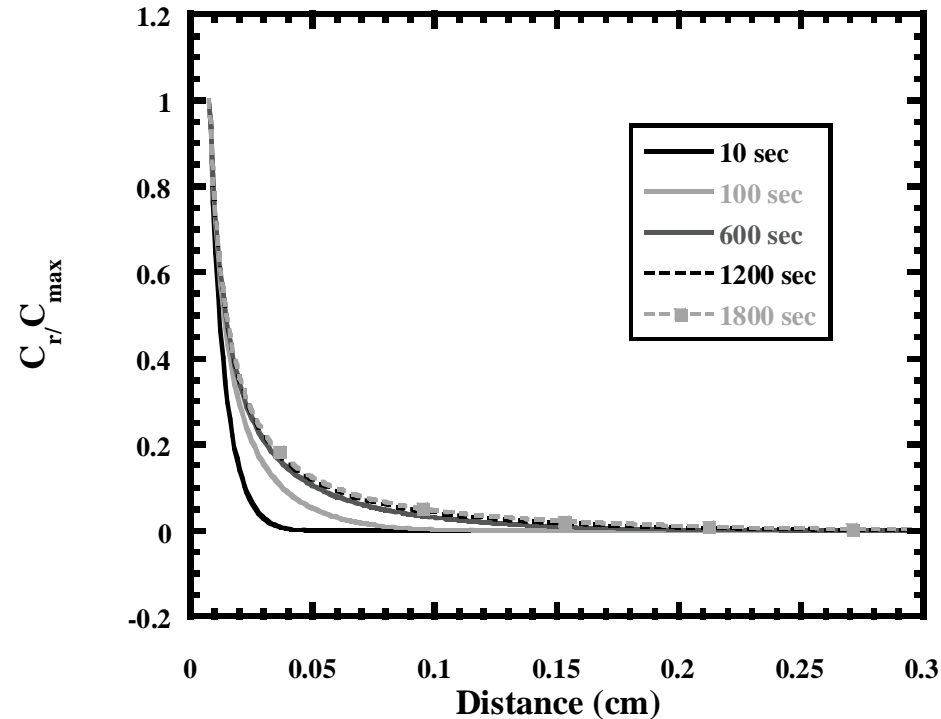
a = radius of the pit (cm)

r = radial distance away from the pit mouth (cm)

erfc = complementary error function

D = diffusion coefficient of the diffusion ion (cm^2/s)

t = time (seconds)



Current Distributions on Coupled Electrode Array Surfaces

$$\sum I_{Anodic} = \sum I_{Cathodic}$$

For any electrochemical system

$$\sum I_{Anodic}^{Applied} = \sum I_{Cathodic}^{Applied} + I_{Cathodic}^{CE_Potentiostat}$$

For an anodically polarized system

Where:

$$\sum I_{Anodic}^{Net_Anode} + \sum I_{Anodic}^{Net_Cathode} = \sum I_{Anodic}^{Applied}$$

$$\sum I_{Cathodic}^{Net_Anode} + \sum I_{Cathodic}^{Net_Cathode} = \sum I_{Cathodic}^{Applied}$$

A portion of the anodic and cathodic current come from both the net anode and net cathode.

$$\sum I_{Anodic}^{Net_Anode} + \sum I_{Anodic}^{Net_Cathode} = \sum I_{Cathodic}^{Net_Anode} + \sum I_{Cathodic}^{Net_Cathode} + I_{Cathodic}^{CE_Potentiostat}$$

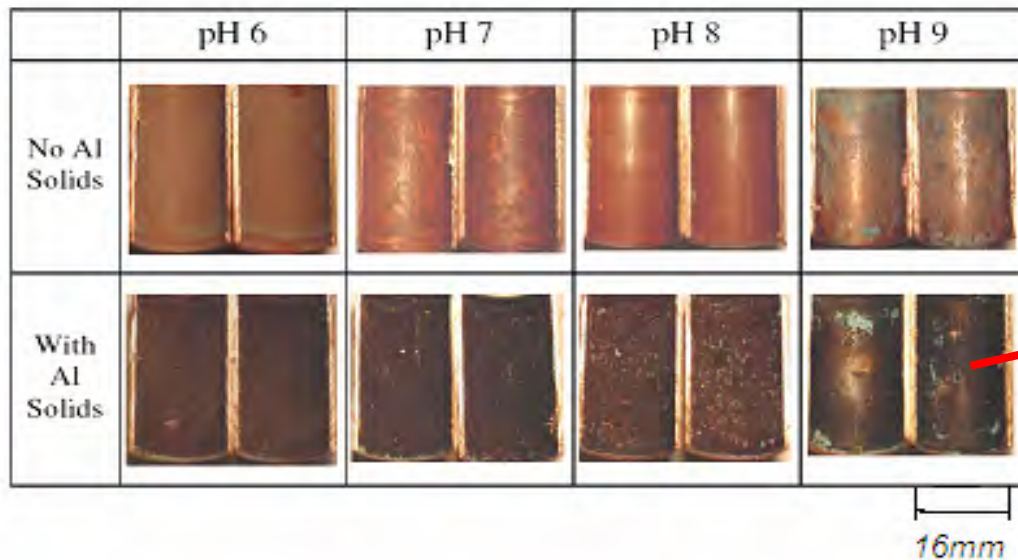
On each electrode element the measuring ZRA either measures a net anode or net cathode. However, local anodes and cathodes are possible.

$$\left(\sum I_{Anodic}^{Net_Anode} - \sum I_{Cathodic}^{Net_Anode} \right) = \left(\sum I_{Cathodic}^{Net_Cathode} - \sum I_{Anodic}^{Net_Cathode} \right) + I_{Cathodic}^{CE_Potentiostat}$$

The net current for each wire, either net anodic or net cathodic, is what is measure by the ZRA.

Interplay between Water Chemistry and Electrochemical Properties of Copper

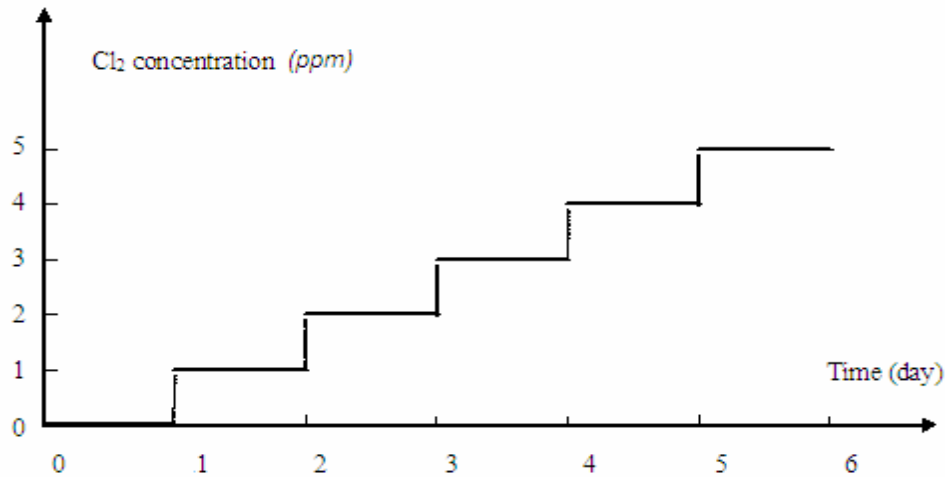
- Study the fundamental mechanism of copper pitting, elucidate electrochemical properties as a function of: chlorine, aluminum, pH, sulfate, chloride, susceptible v.s. unsusceptible waters etc.
- Circumstantial evidence of susceptible water chemistries emerging but not firmly linked to key electrochemical properties associated with pitting;
- High PH: from pH = 8 to somewhere below PH = 10;
- High Chlorine (5 ppm) and High Aluminum (2 ppm Al-Al(OH)₃) accelerate copper pitting by synergistic reactions that cause potential rise and accelerated chlorine reduction.



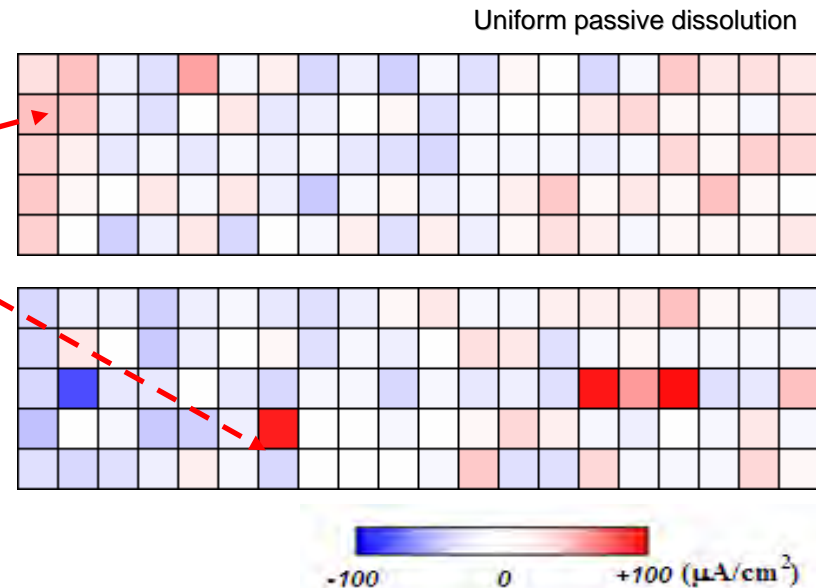
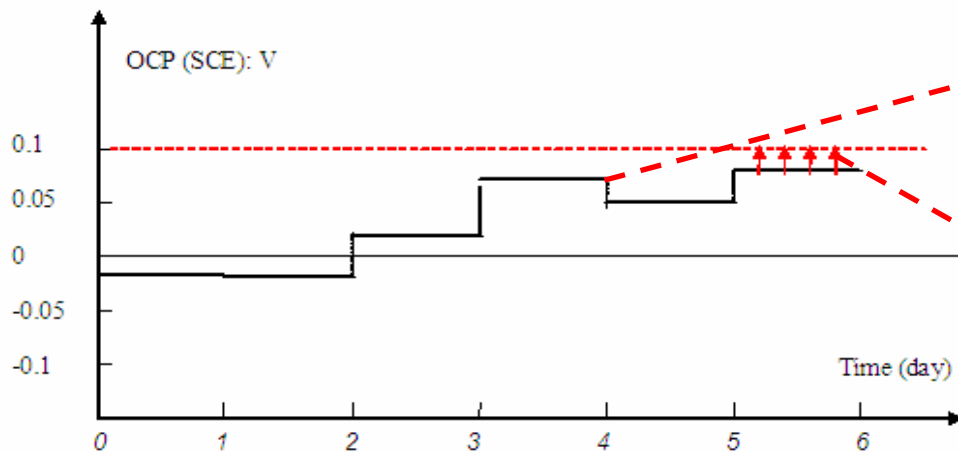
Marshall, 2004

Need: Investigate the spatial development of persistent or switching local anodes as a function of water chemistry.

Development of Local Anodes



Close packed array was set up in flat cell to simulate the vertical inside of copper pipe. 2 ppm Al-Al(OH)₃ was added in synthetic water, and pH was adjusted to 9.2. Starting from 0 ppm, Cl₂ was increased by 1 ppm per day to 5 ppm by adding NaClO solution into test water.

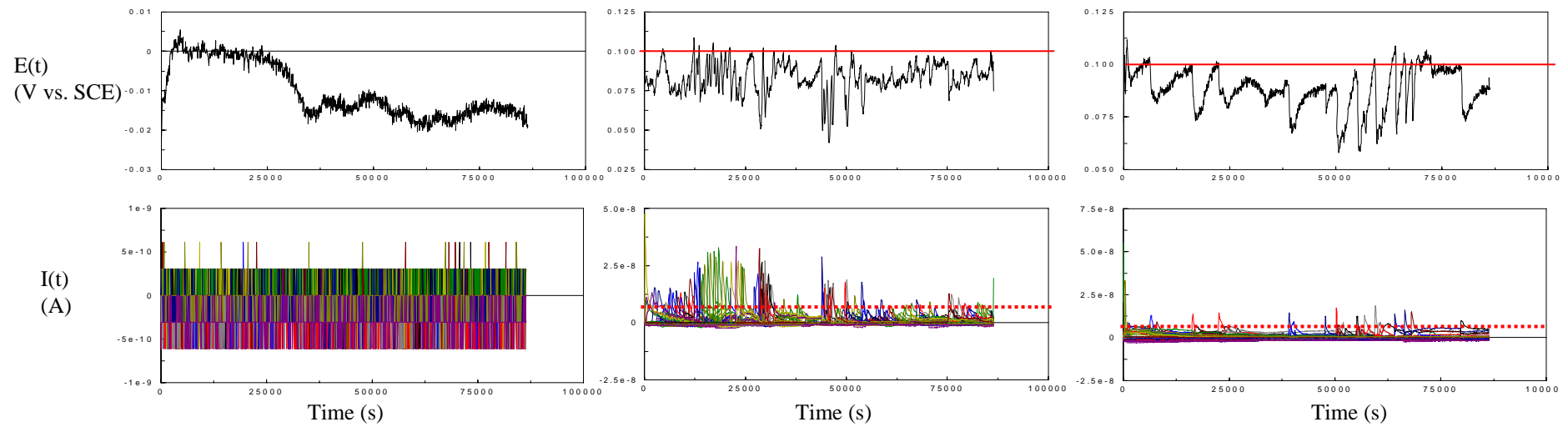


pH = 9 Synthetic Water, 2 ppm Al-Al(OH)₃ added

1 ppm Cl₂

3 ppm Cl₂

4 ppm Cl₂



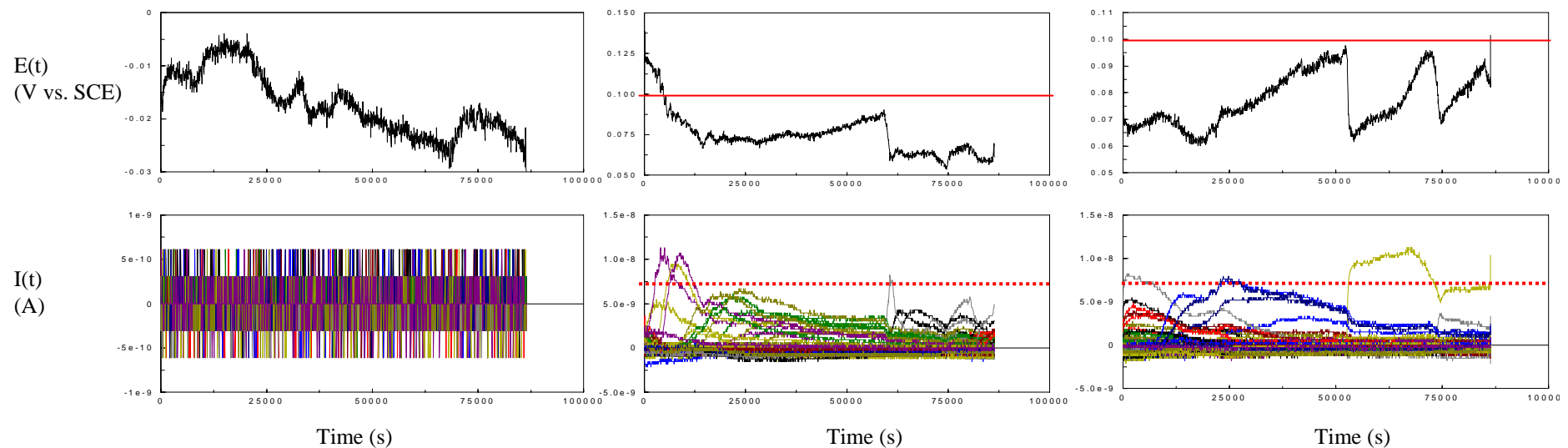
Critical line: Potential: 100 mV (vs. SCE) (solid line); Current density: 40 μA/cm² > 20 mpy (i.e. 200 mpy) (dash line)

pH = 9 Synthetic Water, No Aluminum added

1 ppm Cl₂

3 ppm Cl₂

4 ppm Cl₂

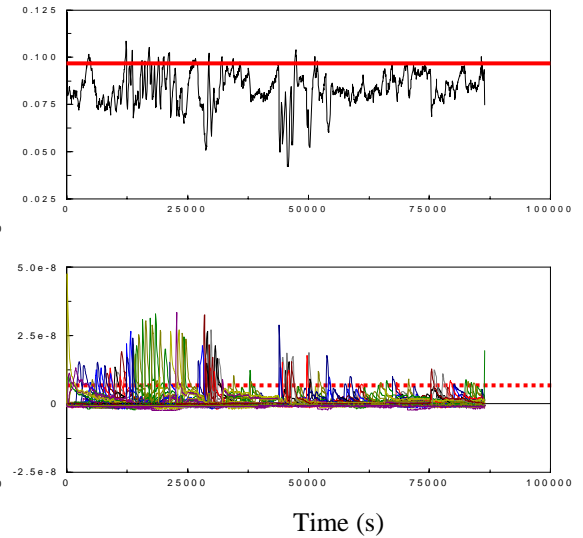
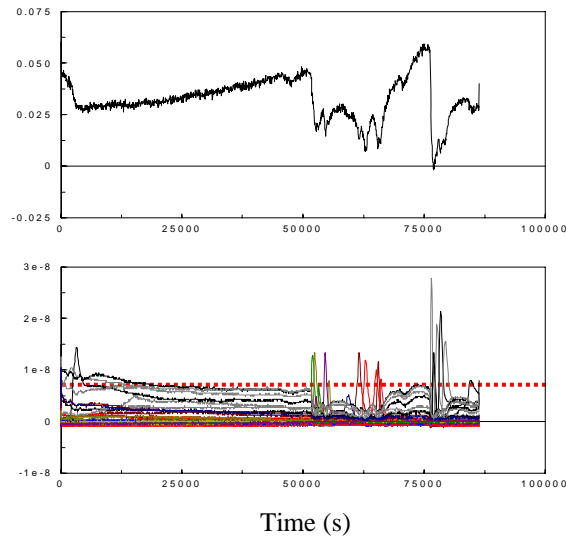
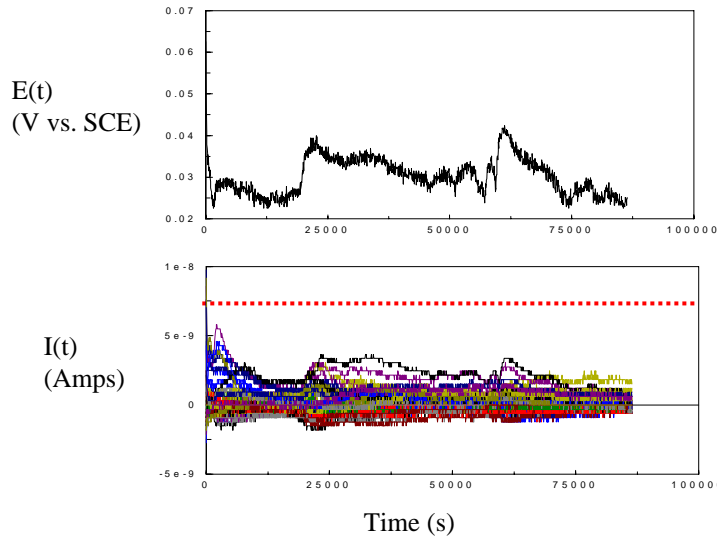


Chlorinated Synthetic Water (3 ppm Cl₂), 2 ppm Al-Al(OH)₃

pH = 6

pH = 8

pH = 9



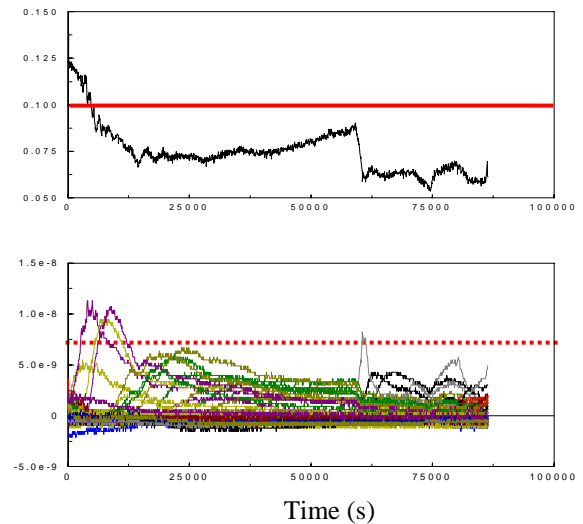
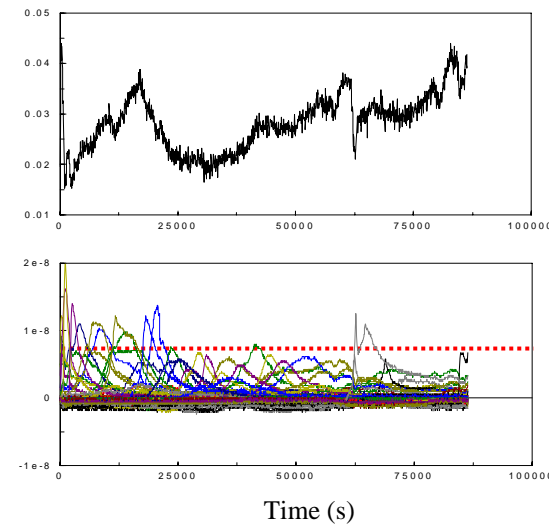
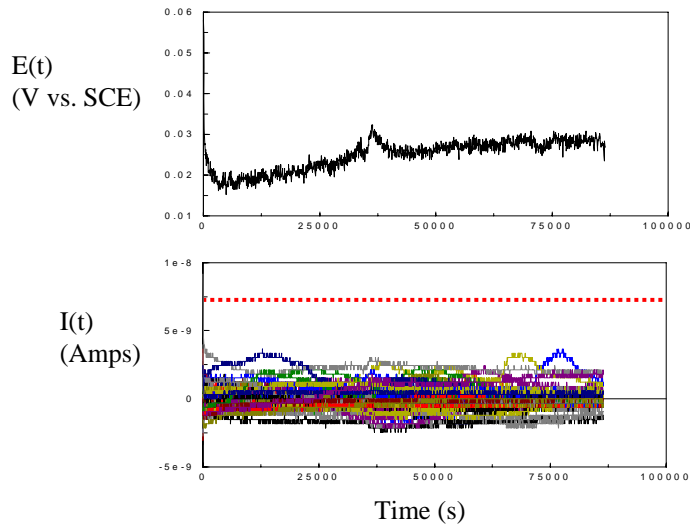
Critical line: Potential: 100 mV (vs. SCE) (solid line); Current density: 40 $\mu\text{A}/\text{cm}^2$ > 20 mpy (i.e. 200 mpy) (dash line)

Chlorinated Synthetic Water (3 ppm Cl₂), No Aluminum added

pH = 6

pH = 8

pH = 9



Conditions for Pit Initiation Identified

Number of Wires with Pitting Events Greater than $40 \mu\text{A}/\text{cm}^2$

No Aluminum in synthetic water

[Cl ₂] (ppm)	pH = 6	pH = 7	pH = 8	pH = 9
5	0	2	2	4
4	9	1	4	4
3	0	0	19	4
2	4	2	21	7
1	0	0	0	0
0	0	0	0	0

2 ppm Aluminum in synthetic water

[Cl ₂] (ppm)	pH = 6	pH = 7	pH = 8	pH = 9
5	0	4	9	11
4	3	2	7	26
3	5	13	24	83
2	0	10	19	0
1	0	2	0	0
0	0	0	0	0

A rapid lab screening method?

Criterion:

The current density measured on a single wire exceeded $40 \mu\text{A}/\text{cm}^2$ (20 mpy) at least once during the test;

If 1/10th of area pitted, then >200 mpy

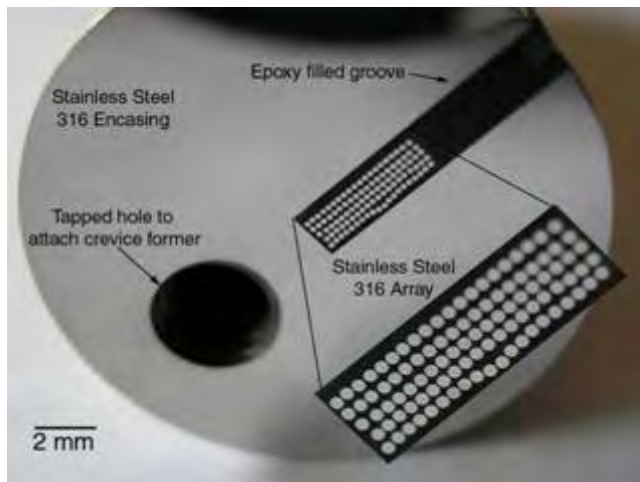
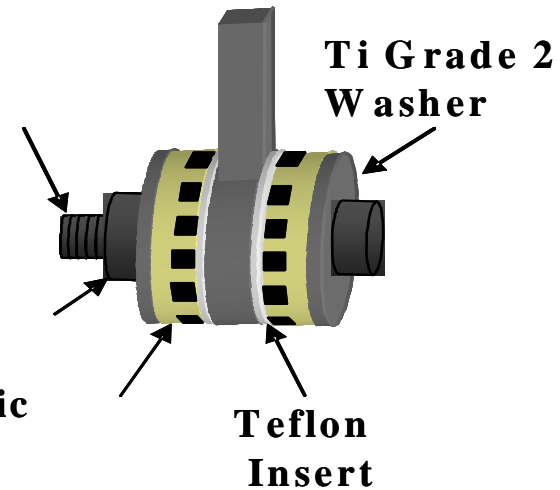
Multi-Crevice Assembly vs. MEA

- The array is flush-mounted in a metallic rod of the same material, resulting in a metallic surface-volume ratio similar to that of MCA
- Array provides detailed spatial-temporal resolution, important as crevice corrosion behavior is very dependant on position
- Easier study of effects on initiation and propagation of some factors such as: proximate cathode, limited cathode and semi-permeable crevice former

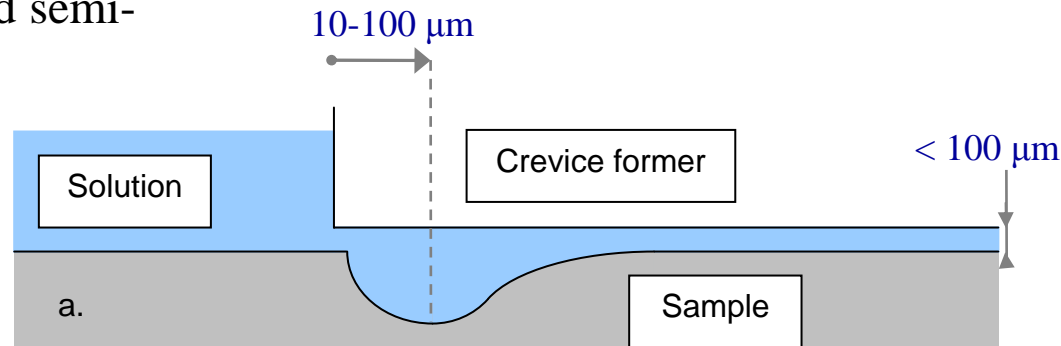
**Insulated
Ti Grade 2 Bolt**

Ti Grade 2 Nut

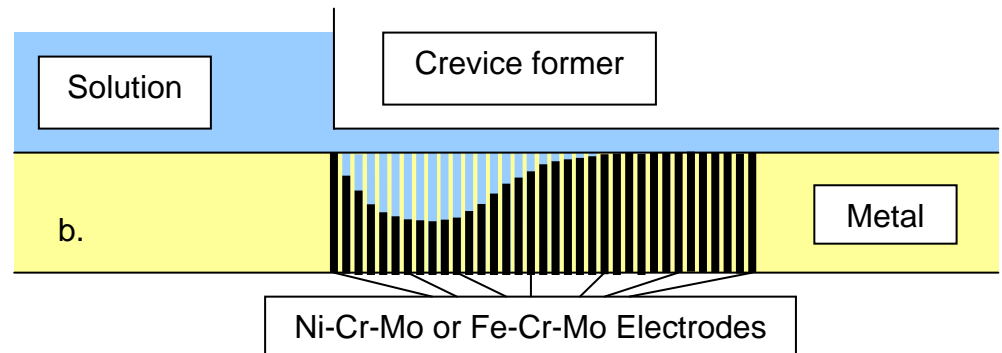
**Serrated Ceramic
Crevice Washer**



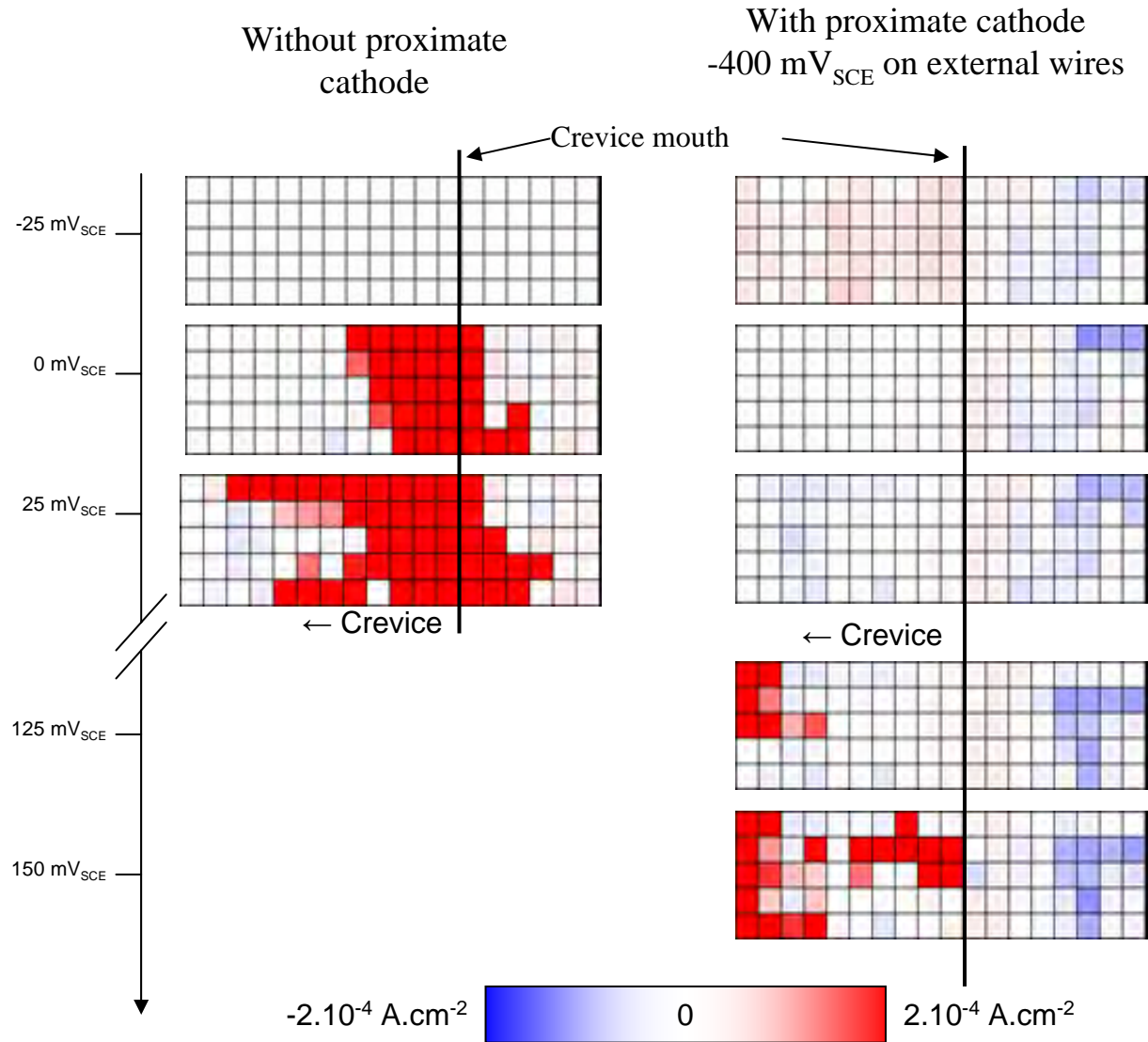
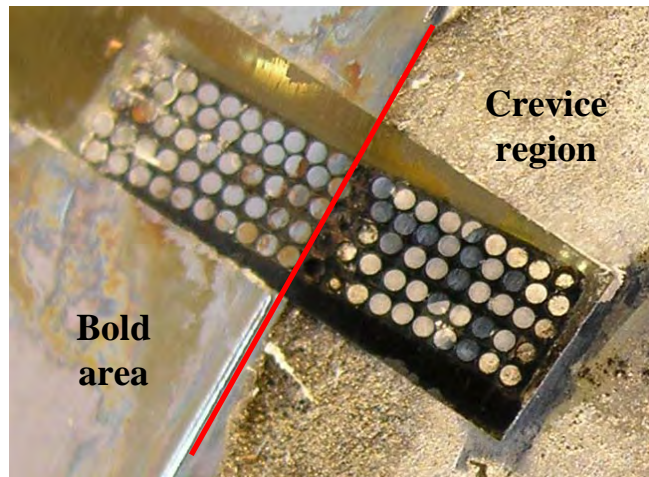
MCA



MEA



Crevice Corrosion & Proximate Cathode



- Setup (316 SS Array) 0.6 M NaCl; aerated; 50°C; 25 in-lbs torque
- 2 days at OCP; 25 mV/day increments up to 150 mV_{SCE}; Initiation at 125 mV_{SCE}.
- Outside wires at -400 mV_{SCE}

Proximate limited cathode inhibits crevice corrosion initiation, in the case of a thin film solution.

Crevice Corrosion Analysis

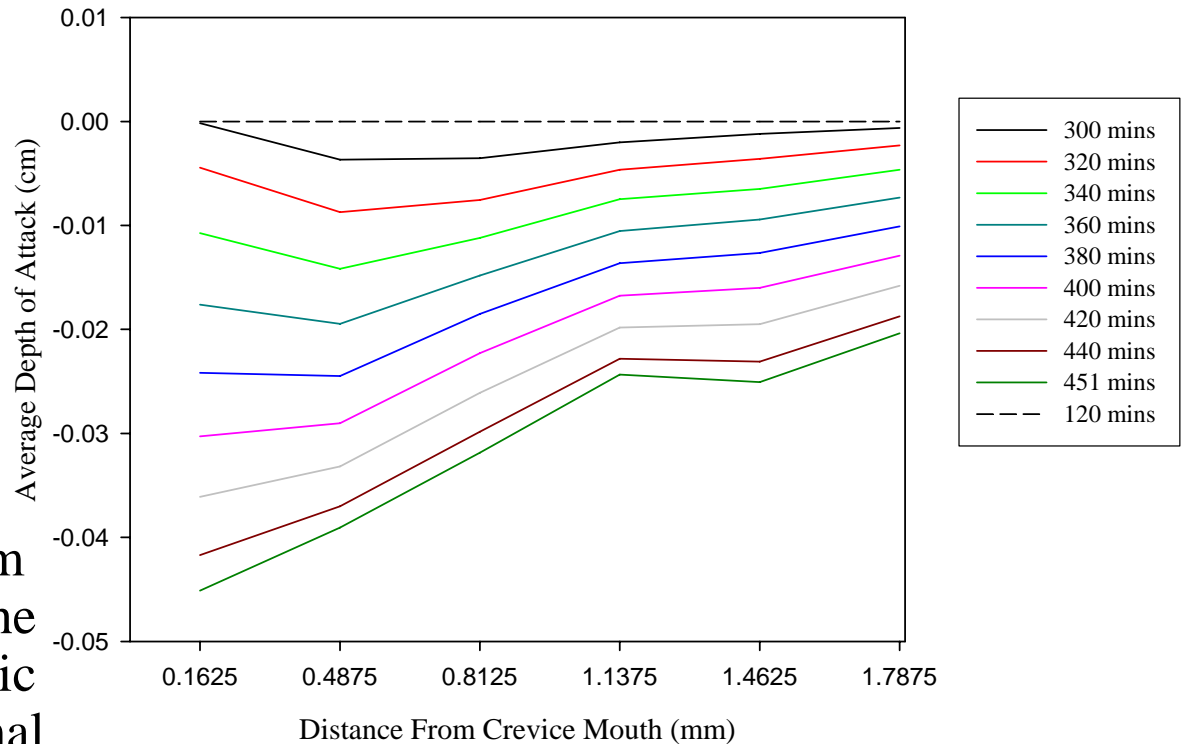
- From Faraday's Law:

$$d = \frac{C \cdot EW_{316SS}}{F \cdot \rho_{316SS} \cdot \pi \cdot r^2}$$

With $EW_{316SS} = 25.4$

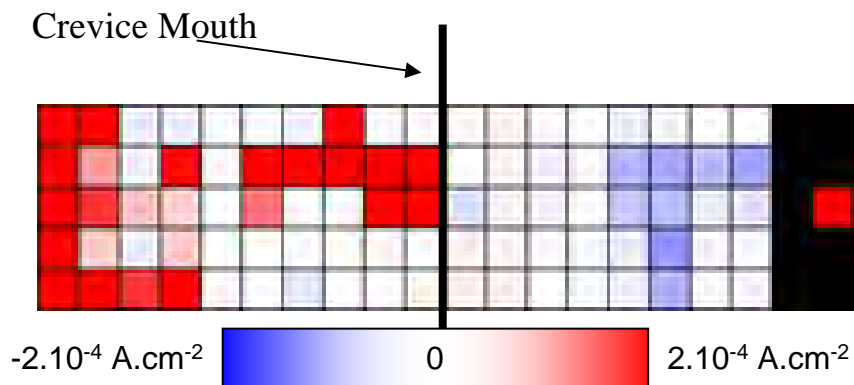
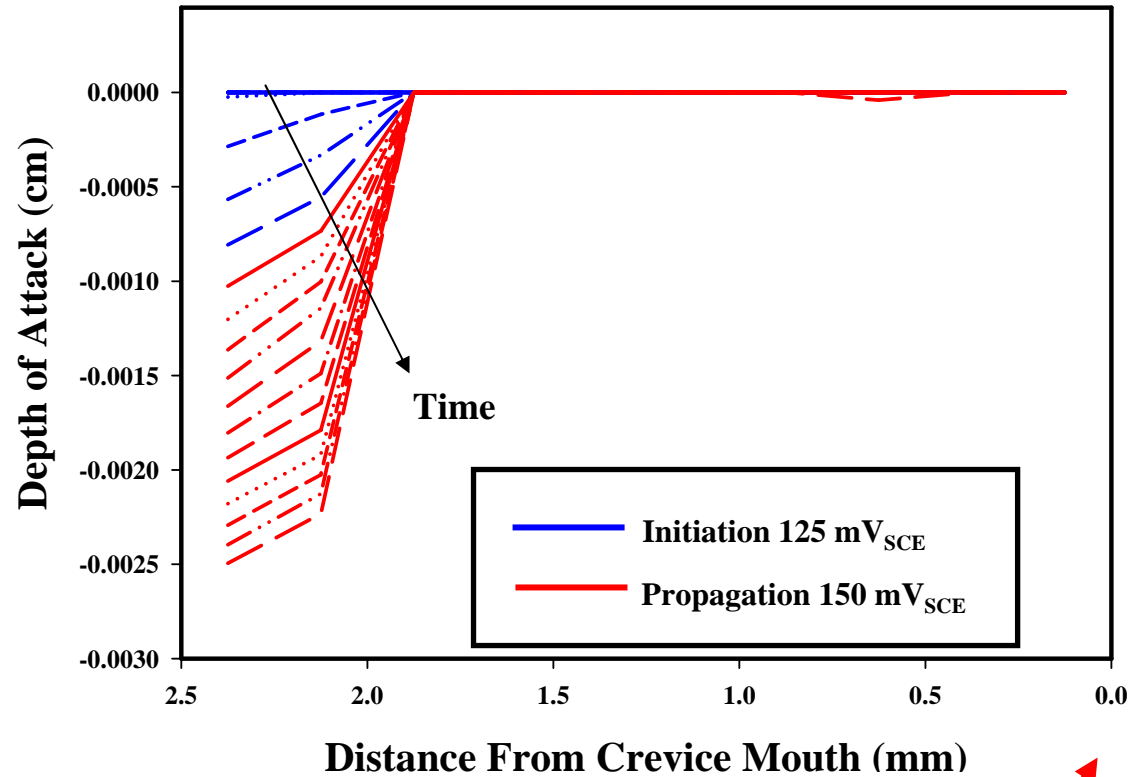
and $\rho_{316SS} = 7.87$

- The charge is derived from the net current. Close to the crevice mouth, the cathodic current part will be minimal
- The derived depth of attack profile evolution is in agreement with the IR drop model



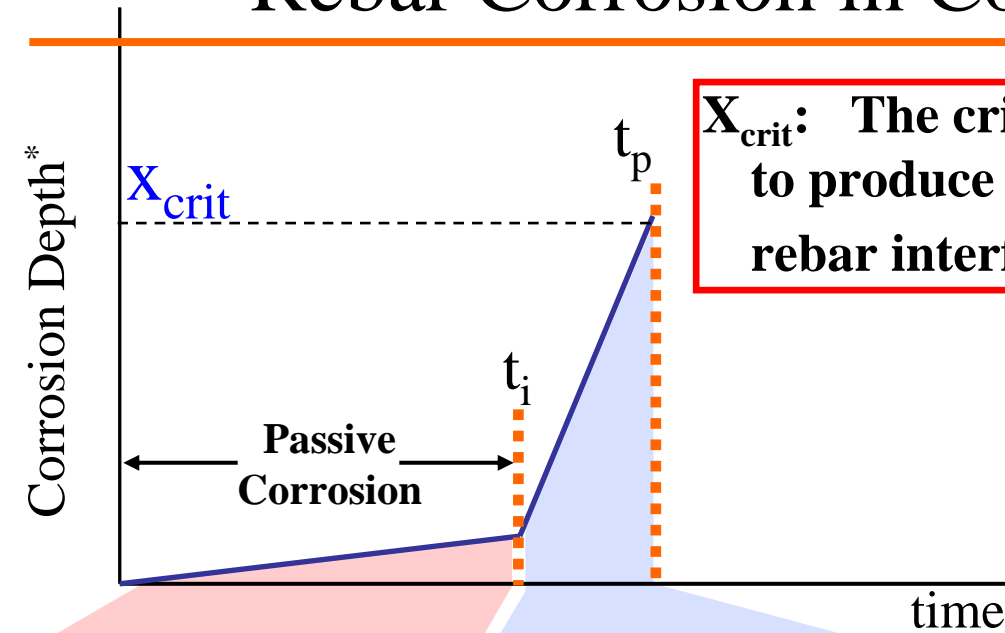
Proximate Cathode: Zone of Attack

The proximate cathode, located outside the crevice mouth inhibits crevice corrosion from forming close to the mouth opening. Deep within the crevice mouth crevice corrosion initiates and propagates towards the mouth.

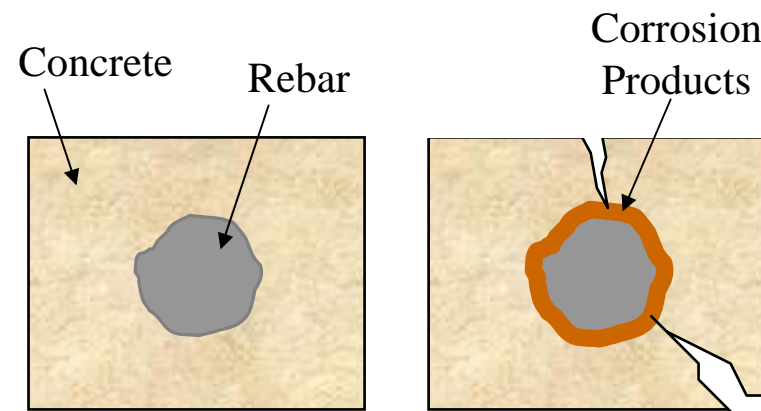


Crevice Mouth

Rebar Corrosion in Concrete: Background



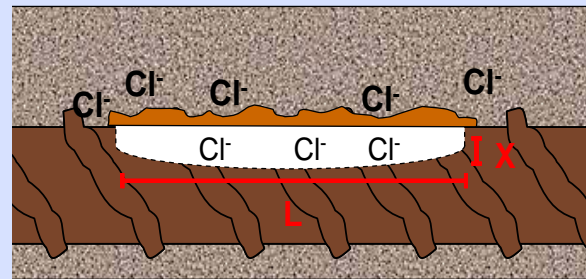
X_{crit} : The critical depth of corrosion attack required to produce sufficient corrosion products at the rebar interface to crack the surrounding concrete



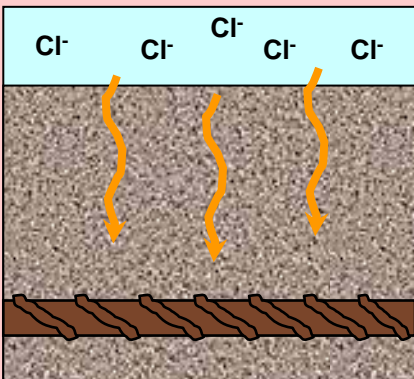
Time to Spalling

(when $X > X_{crit}$)

$$t_{failure} = t_i + t_p$$



t_p = alloy quality, corrosivity environment, electrochemical conditions



t_i = concrete quality, alloy composition

*After: K. Tuutti, *Corrosion of Steel in Concrete*. Swedish Cement and Concrete Research Institute: Stockholm. p. 18,51, 1982.

Corrosion Propagation: Impact on Concrete Structures

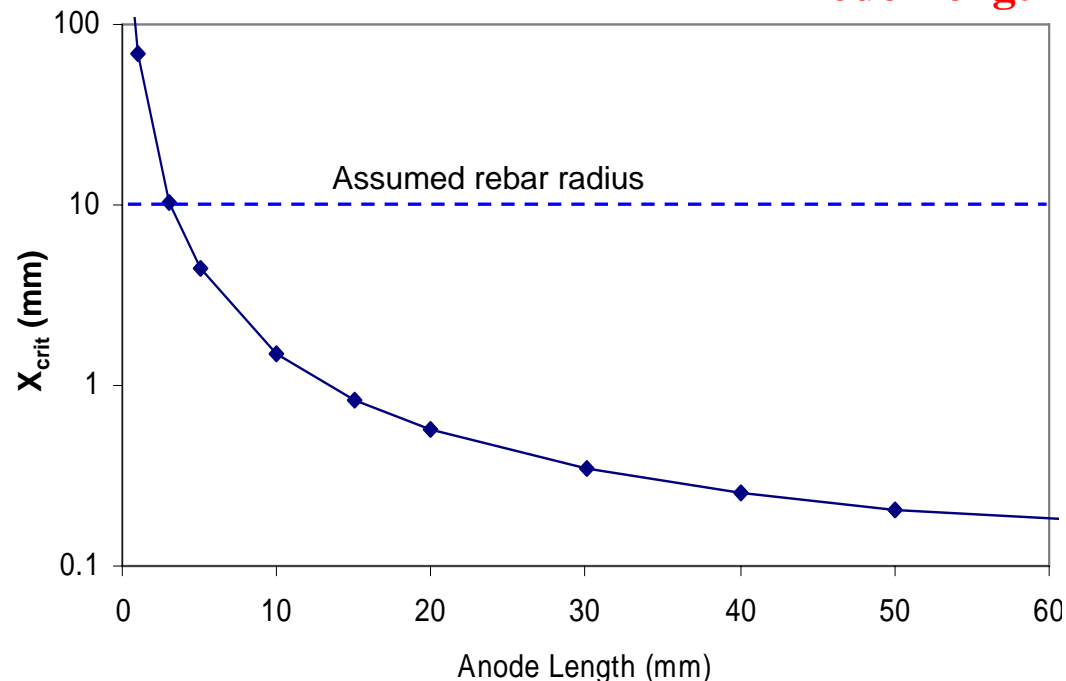
x_{crit} = Corrosion Depth Required to Damage Concrete

- **Degree of localization impacts concrete cracking**
 - For carbon steel an empirical relationship has been found*
- **Effect of new rebar alloys**
 - Higher aspect ratio corrosion morphology
 - Unique metal-to-oxide conversion rate
 - **MEA's utilized to study anode length of new rebar alloys developed during lateral growth of corrosion damage**

$$x_{crit} = 0.011 \left(\frac{C}{\phi} \right) \left(\frac{C}{L} + 1 \right)^{1.8}$$

Concrete Cover $C = 50$ mm
Rebar Radius $\phi = 10$ mm

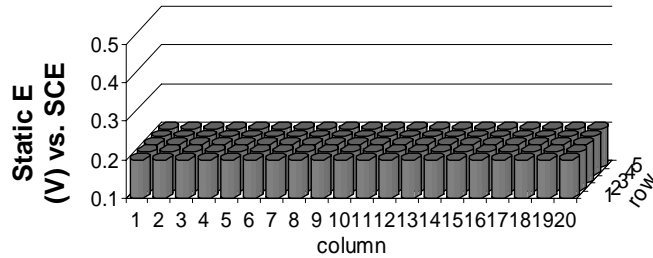
Anode Length



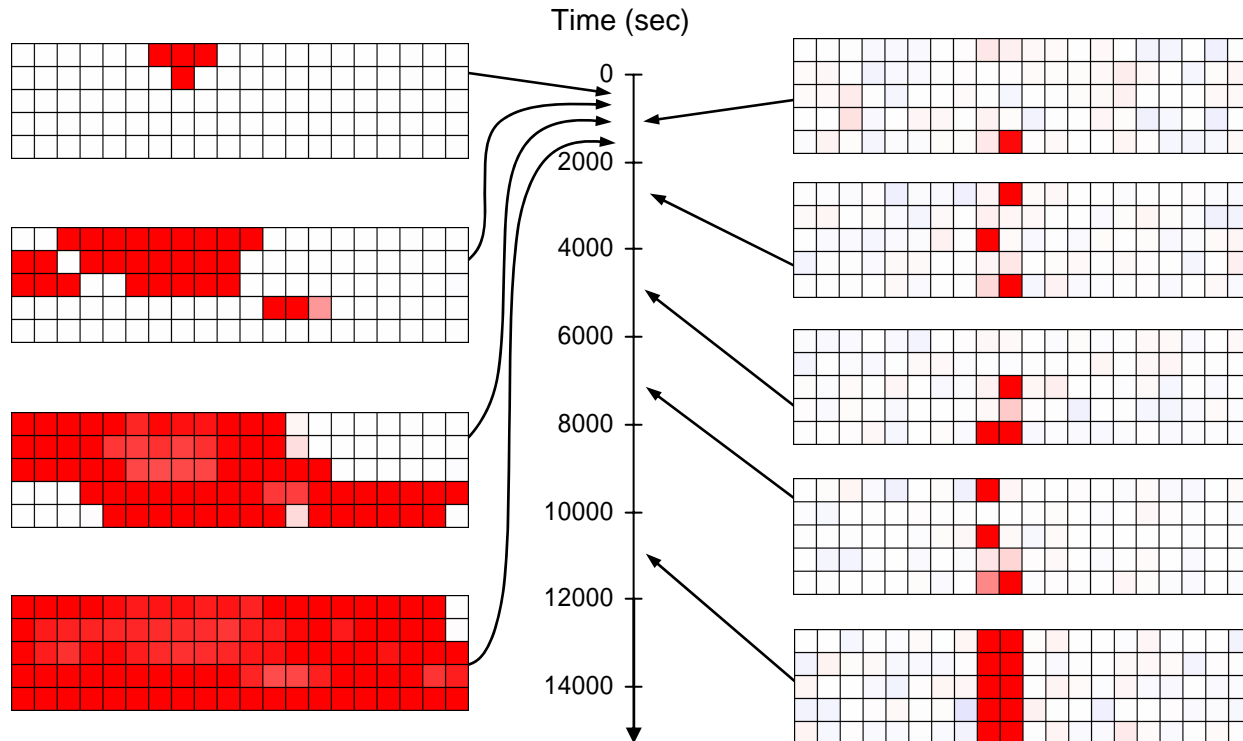
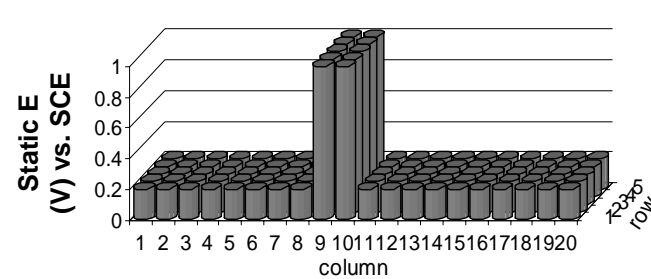
*A.A. Torres-Acosta and A.A. Sagues. Concrete Cover Cracking with Localized Corrosion of Reinforcing Steel. In 5th CANMET/ACI. 2000. Barcelona: ACI Intl.

Corrosion Propagation: Lateral Spreading

Carbon Steel: Corrosion spreads rapidly across the MEA surface



316L Stainless Steel: No spreading is seen from preferentially activated sites

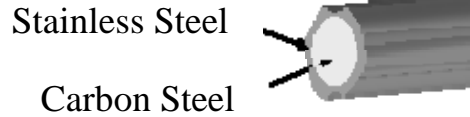


Carbon Steel Saturated
 $\text{Ca}(\text{OH})_2 + 0.2 \text{ M NaCl}$

316L Stainless Steel $\text{H}_2\text{O} + 3 \text{ M NaCl}$

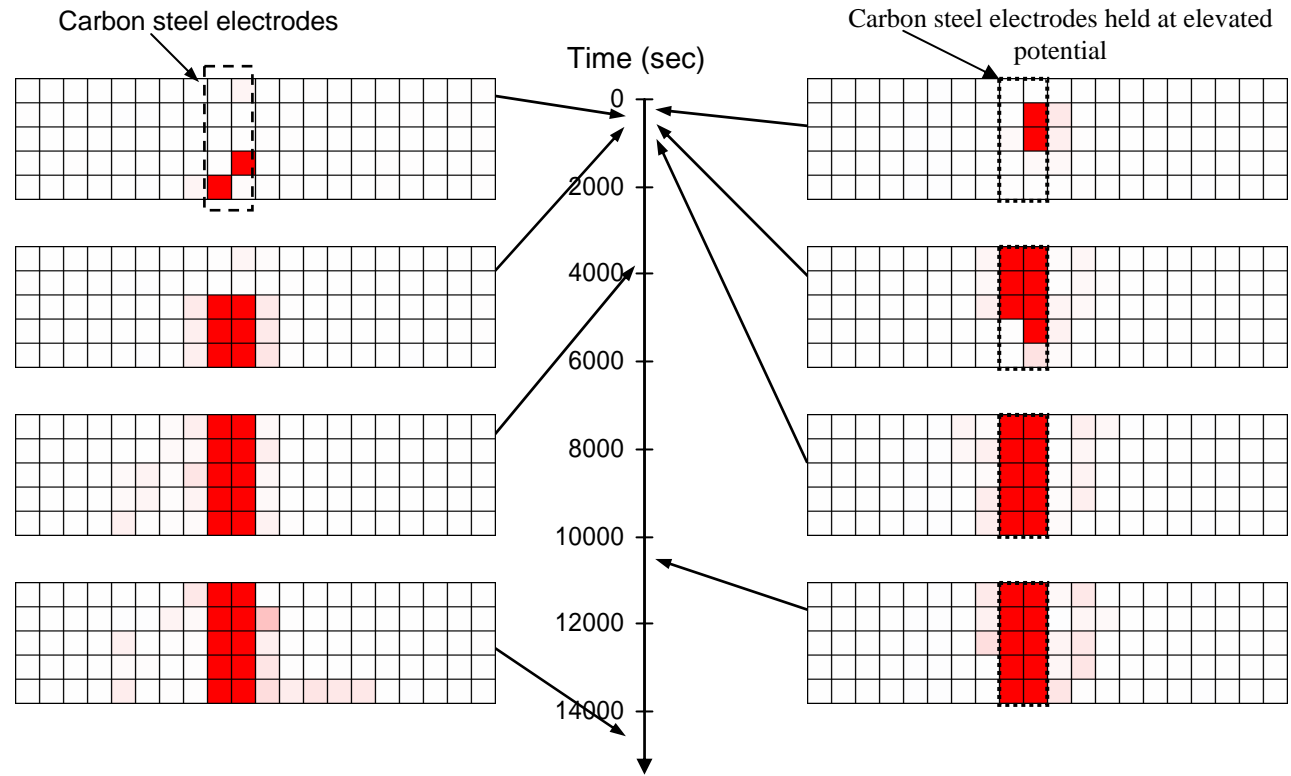
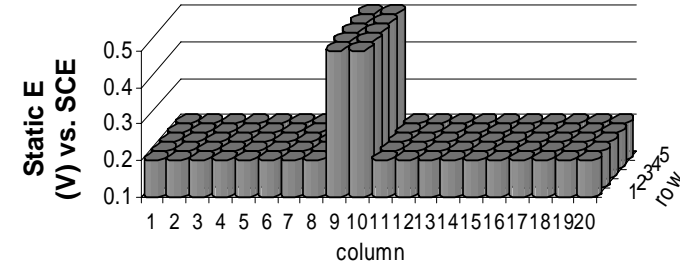
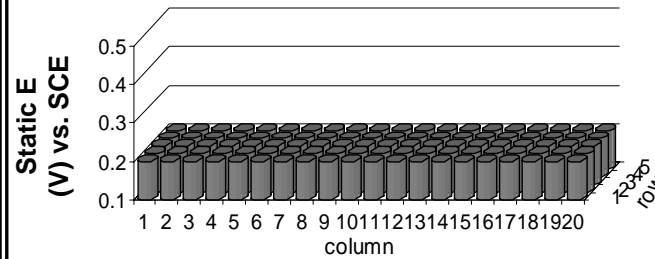
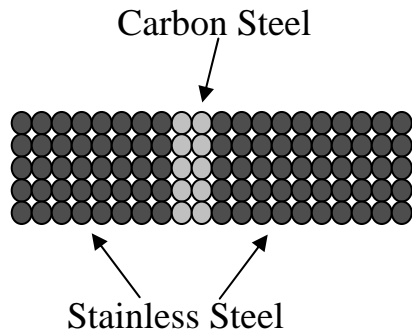
Corrosion Propagation: Simulated Clad Rebar

Clad Rebar



•An MEA was constructed to simulate a “defective” Stainless Steel clad over carbon steel rebar

•Can corrosion at the breach propagate to the clad layer?



Simulated Clad
Sat. $\text{Ca}(\text{OH})_2 + 0.2\text{M NaCl}$

Simulated Clad
Sat. $\text{Ca}(\text{OH})_2 + 0.2\text{M NaCl}$

Spreading of Intergranular Corrosion by Cooperative Interactions



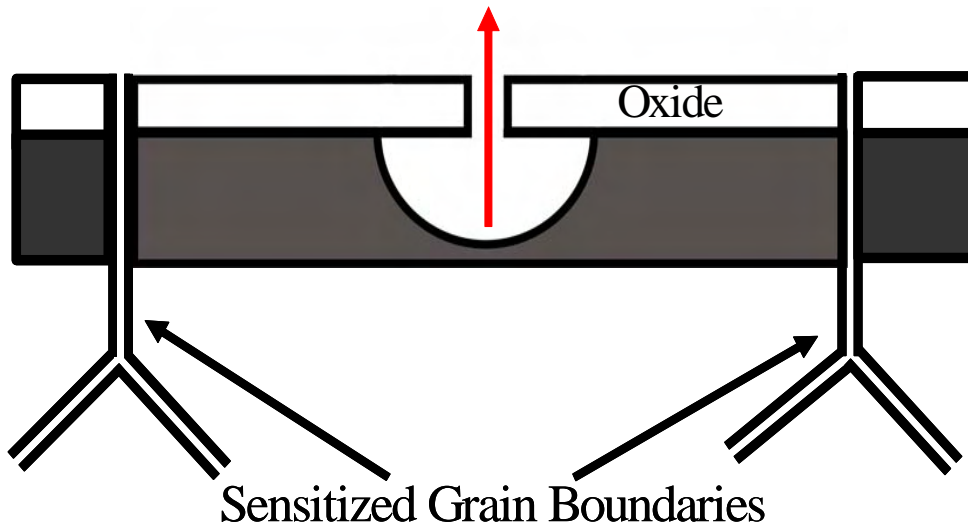
Ohmic Potential Shielding (Enhance)



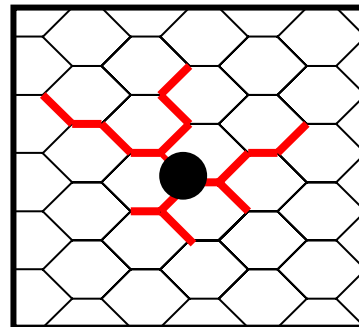
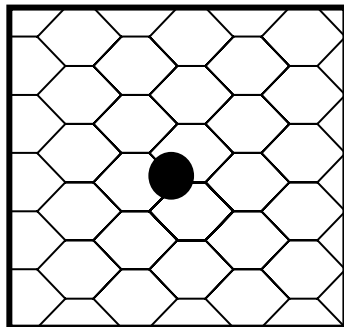
Aggressive Species Enhancement (Enhance)



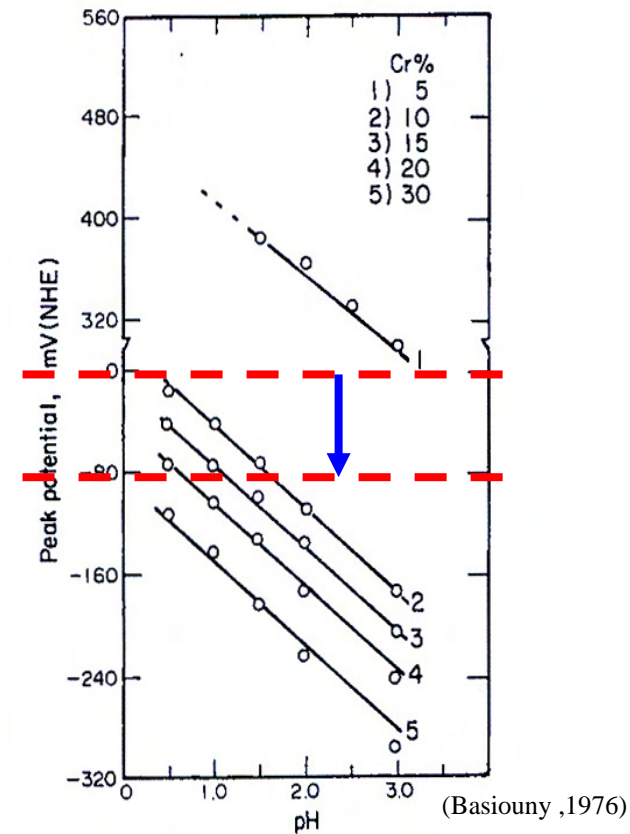
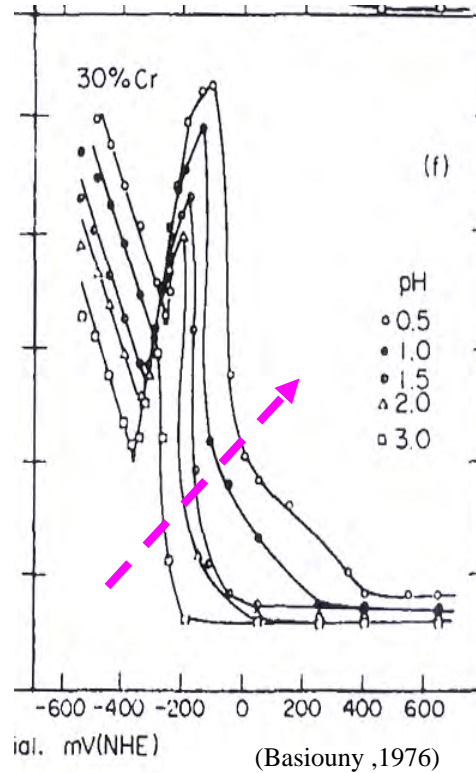
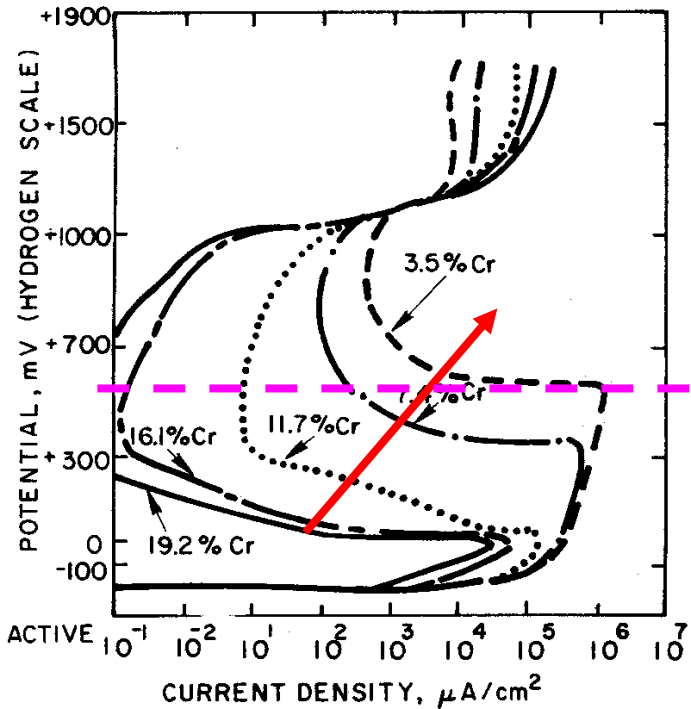
Persistent Surface Damage (Enhance)



- The triggering of intergranular corrosion on sensitized stainless steels from pitting sites.
- Self propagating growth of accumulated IGC damage across electrode surfaces.



Initiation of IGC From Localized Pitting



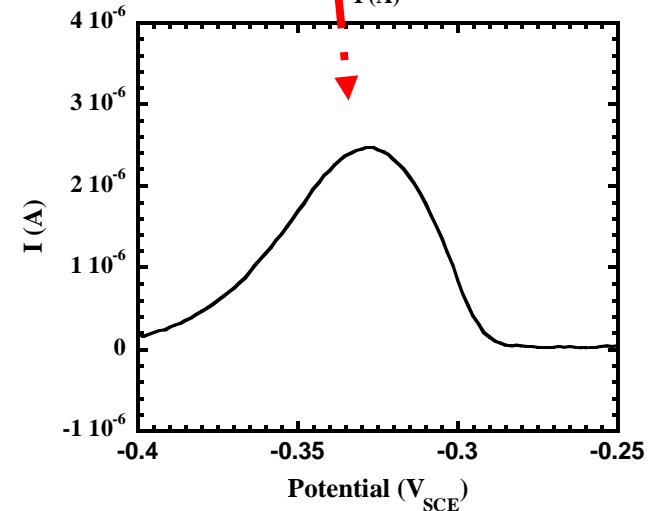
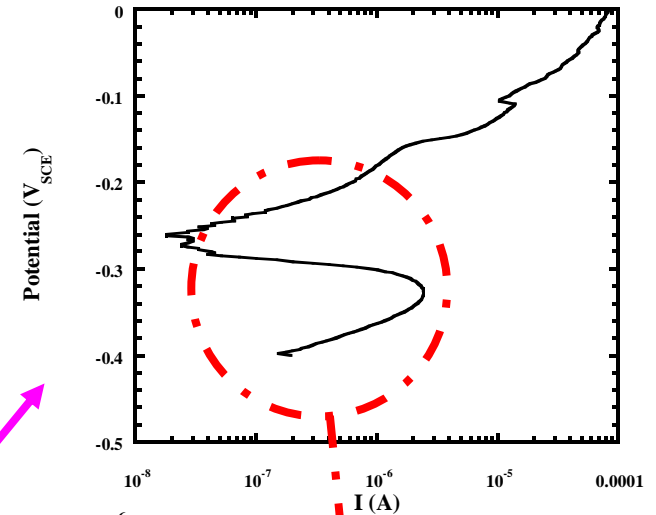
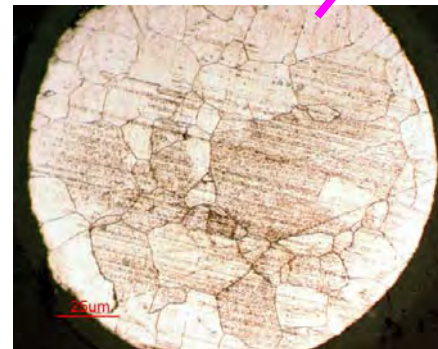
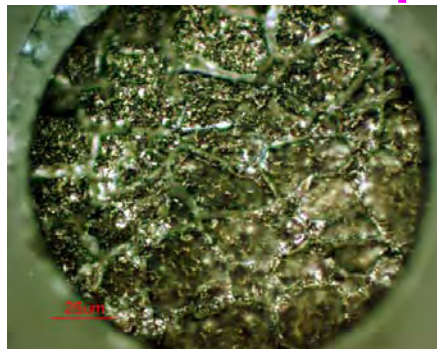
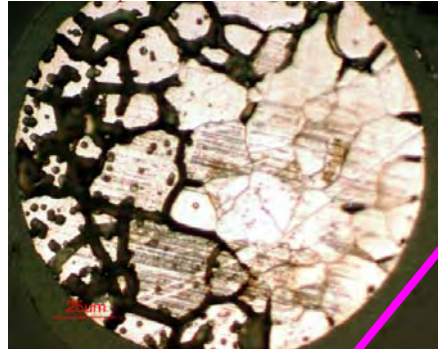
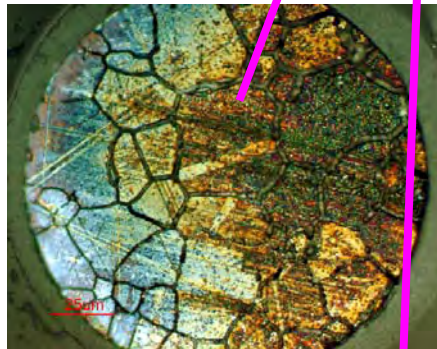
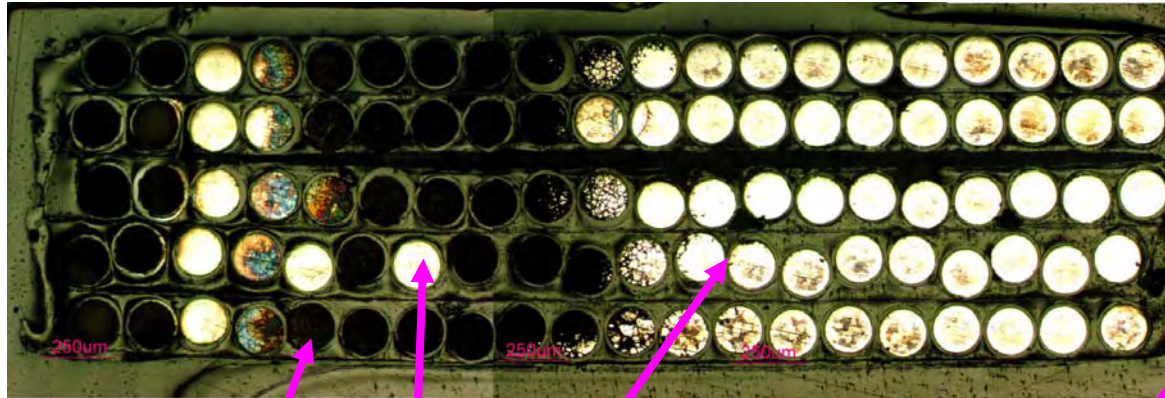
(Osozawa, 1966)

- E_{Flade} increases with decreasing [Cr].
- E_{Flade} increases with decreasing pH.
- G.B. with lowest [Cr] most susceptible to initiation and continued growth.

Ohmic potential can be generated in solution originating from pits or from grain boundaries that are undergoing IGC.

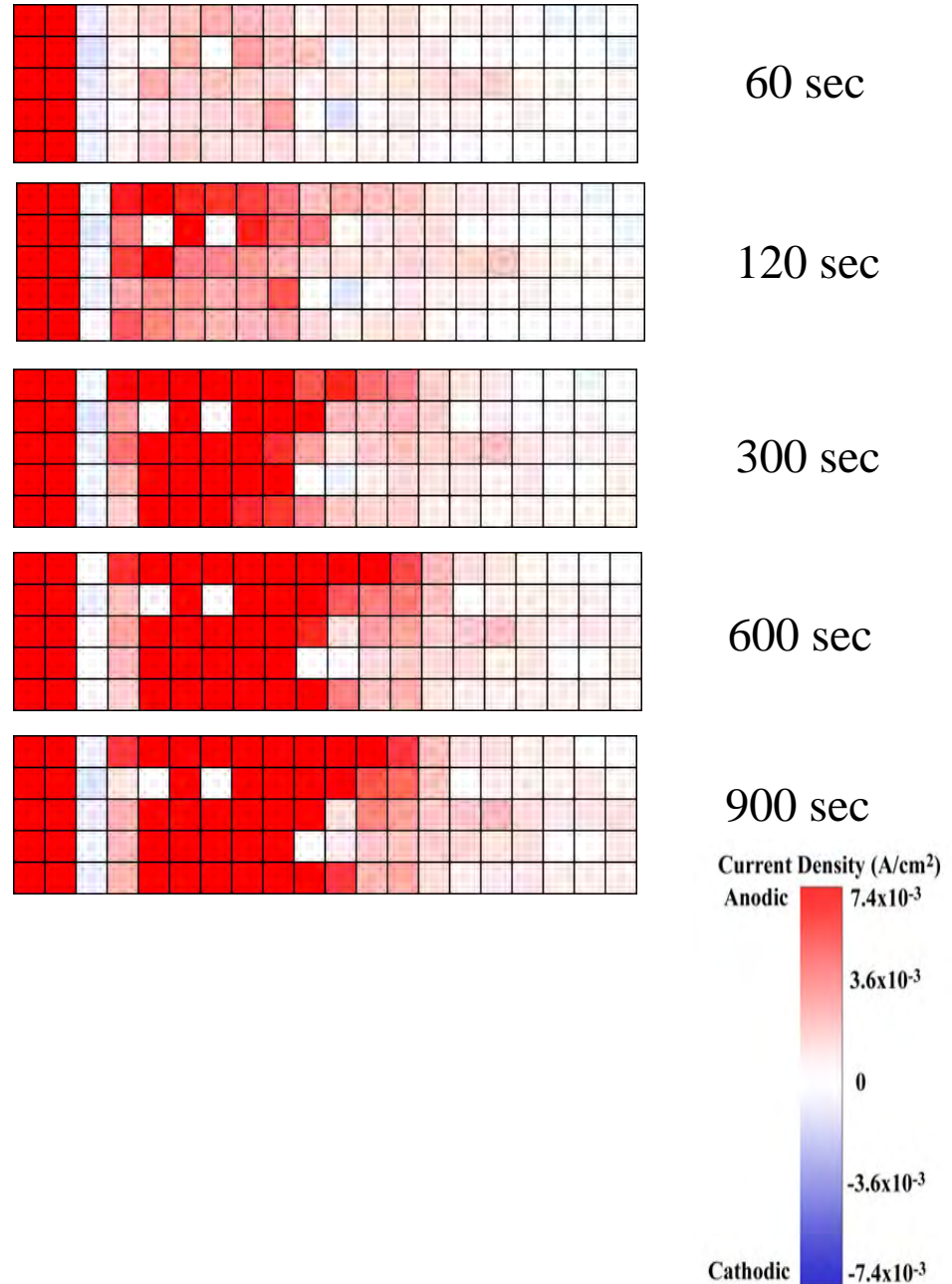
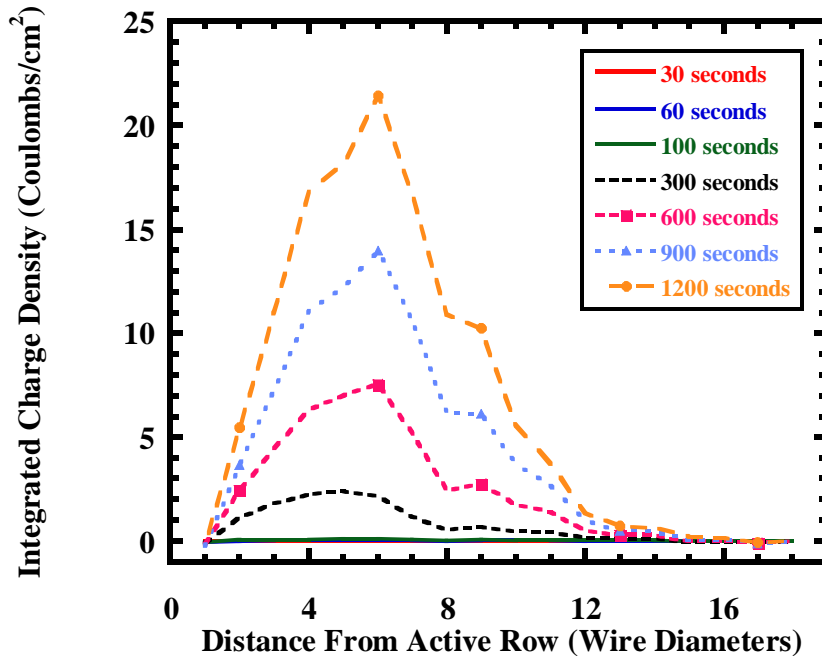
Ohmic potential can cause the applied potential on surrounding surface to drop from a passive potential into an active range

Pits trigger IGC on sensitized stainless steel



- Sensitized 304 (1030°C 1 hour and 621°C 48 Hrs) in 0.06 M HCl 60°C
- Induced interaction experiments: Rows 1 and 2 (1 V_{SCE}) and remaining electrodes (-0.29 V_{SCE})

Measured Accumulated IGC Damage



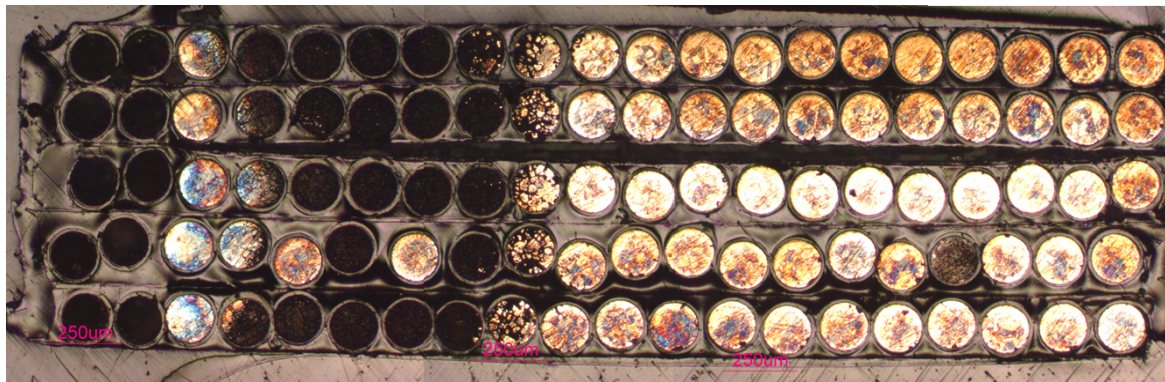
- **Visually observed accumulated damage matches current and charge measured with MEA.**
- **Damage spreads with time beyond predicted region of accumulated damage by ohmic potential drop-solution enhancement**

Separation of Cooperative Interaction Mechanisms



Without Stirring

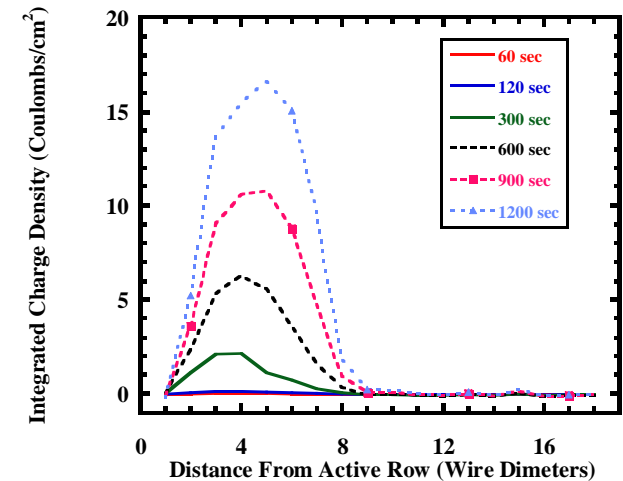
- Ohmic Potential Drop
- Solution Enhancement



With Stirring

- Ohmic Potential Drop

- From previous experiments involving pitting corrosion it was found that concentration fields had significant effects within 3-4 wire diameters. In the unstirred case these wires are farther away then 3-4 rows thus concentration fields are supplied by wires that are undergoing IGC. This implies that IGC can be autocatalytic under certain conditions.



Predicted Regions of IGC From Ohmic Potential

- Using Newman's solution for a disk in an insulator we can predict the ohmic potential drop produced by active pitting.

$$\frac{\Phi}{\Phi_0} = 1 - \left(\frac{2}{\pi}\right) \cdot \text{atan}(\xi)$$

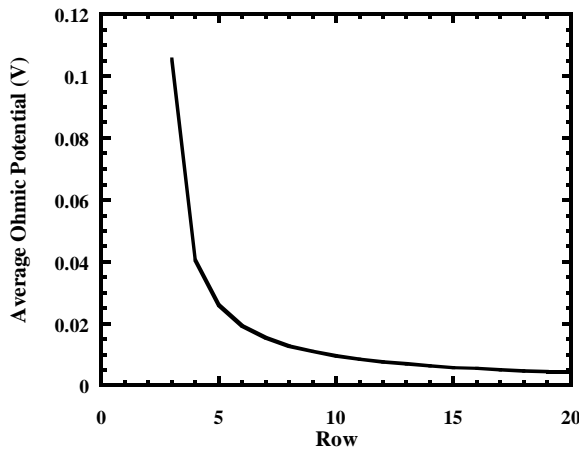
$$I = 4K \cdot r_0 \cdot \Phi_0$$

$$r = r_0 \cdot \sqrt{\left(1 + \xi^2\right) \cdot (1 - \eta)^2}$$

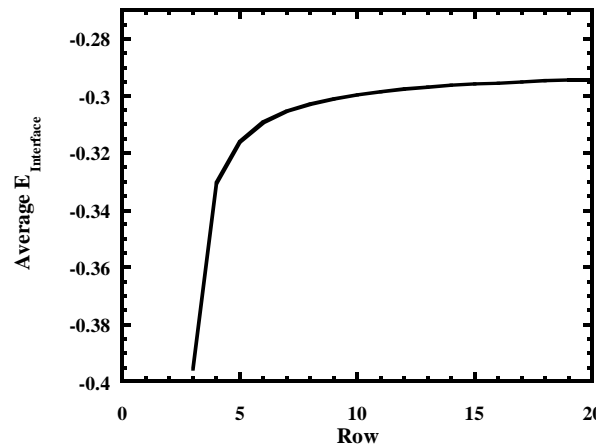
- Assume that an array is a radial slice of this model.
- Using these equations, some experimental values, and potentiodynamic curves the region of IGC damage can be predicted.

$$I = 1.25 \text{ A/cm}^2$$

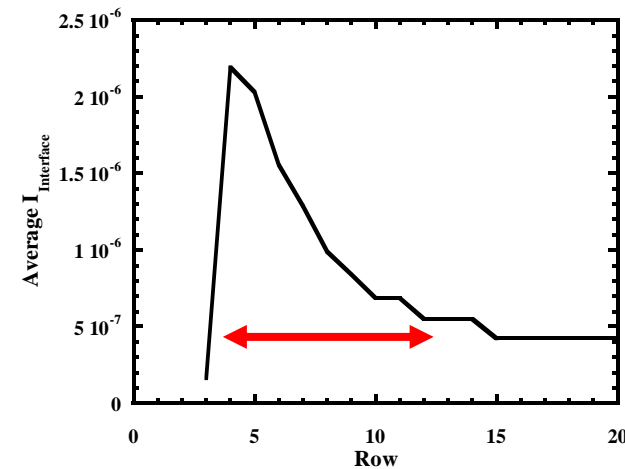
$$K = 0.027 \text{ ohm}^{-1}\text{cm}^{-1}$$



V_{ohmic}



$E_{\text{Interface}} = E_{\text{applied}} - V_{\text{ohmic}}$



Predicted Region of IGC

Conclusions

- MEAs enable the study of water chemistry conditions for initiation of local persistent anodes compared to those that favor uniform dissolution.
 - Synthetic water containing 2 ppm aluminum shows a specific set of conditions where pit initiation occurs
 - Interrogation of local anodes and cathodes possible
- MEAs enables study of crevice corrosion initiation and propagation with unprecedented fidelity
 - Sites of initiation
 - Propagation rates
 - Damage morphology
 - Role of proximate cathodes, unconventional crevices
- MEAs enable the determination of anode lengths for different high performance rebar materials caused by the propagation and growth characteristics of the material. The lateral growth behavior of these materials is crucial to material performance in concrete and monitored in real-time using MEAs.
- Pitting corrosion can trigger IGC on stainless steels through ohmic potential shielding and localized solution enhancement. Lateral growth of IGC can self propagate across electrode surfaces.
 - Material parameters controlling the spreading of IGC can be investigated
 - Physical and environmental parameters can also be investigated

Questions?

Acknowledgements

- **The concrete project was sponsored by the VTRC (Virginia Transportation Research Council). The support and helpful discussions with Dr. Gerardo Clemenña and Dr. Steve Sharp are gratefully acknowledged.**
- **The crevice corrosion work was supported by the Office of Science and Technology International (OST&I), Office of Civilian Radioactive Waste Management, U.S. Department of Energy.**
- **Dr. Harold T. Michels and Copper Development Association Inc. provided financial support for pitting of Cu studies.**
- **The United States Department of Energy, Office of Basic Energy Sciences, Division of Materials Sciences and Engineering supported intergranular corrosion studies under contract DEFG02-00ER45825 with Jane Zhu as contact monitor.**
- **Special thanks to Scribner Associates, Inc. for instrument and software support.**